Soliton refraction by an optical soliton gas

Pierre Suret, Martin Dufour, Giacomo Roberti, Gennady El, François Copie, Stéphane Randoux

Letter

Soliton refraction by an optical soliton gas

Pierre Suret,[1] Martin Dufour,[1] Giacomo Roberti,[2] Gennady El,[2] François Copie,[1] and Stéphane Randoux[1,*]

[1]*Université de Lille, CNRS, UMR 8523 - PhLAM - Physique des Lasers, Atomes et Molécules, F-59 000 Lille, France*

[2]*Department of Mathematics, Physics and Electrical Engineering, Northumbria University, Newcastle Upon Tyne NE1 8ST, United Kingdom*

(Received 24 March 2023; accepted 22 July 2023; published 2 October 2023)

We report an optical fiber experiment in which we investigate the interaction between an individual soliton and a dense soliton gas. We evidence a refraction phenomenon where the tracer soliton experiences an effective velocity change due to its interaction with the optical soliton gas. This interaction results in a significant spatial shift that is measured and compared with theoretical predictions obtained via the inverse scattering transform theory. The effective velocity change associated with the refraction phenomenon is found to be in good quantitative agreement with the results of the spectral kinetic theory of soliton gas. Our results validate the collision rate ansatz that plays a fundamental role in the kinetic theory of soliton gas and also is at the heart of generalized hydrodynamics of many-body integrable systems.

DOI: 10.1103/PhysRevResearch.5.L042002

Solitons are localized nonlinear wave structures that owe their existence to an exact balance between the wave's nonlinearity and the medium's dispersion. Solitons have been observed in a great variety of physical systems including optics [1], matter waves [2,3], fluids [4,5], metamaterials [6], and biophysics [7]. Solitons play a fundamental role in nonlinear physics due to the remarkable property of retaining their shape, amplitude, and velocity upon interactions with other solitons.

The interaction between solitons is a complex nonlinear process that can be understood within the framework of the celebrated inverse scattering transform (IST) developed to solve integrable nonlinear partial differential equations like the Korteweg–de Vries (KdV) equation or the one-dimensional nonlinear Schrödinger equation (1 D-NLSE) [8–12]. Considered on sufficiently large spatiotemporal scales, solitons behave as quasiparticles experiencing short-range pairwise elastic interactions accompanied by well-defined phase/position shifts. The process of elastic collision between two solitons occurs without energy exchange between them and has been studied experimentally in great detail in many physical systems [2,13–22].

Recently, the interaction between an individual (tracer) soliton and a large-scale coherent nonlinear structure such as rarefaction and dispersive shock wave has been studied both theoretically and experimentally [23–29]. The trajectory of the tracer soliton within these macroscopic nonlinear structures is directed by the structure's mean field, which results in either the trapping of the soliton inside or its transmission (tunneling) through the large-scale nonlinear wave.

In this Letter, we present an optical fiber experiment where we examine the interaction between a tracer soliton and a dense soliton gas (SG)—a large ensemble of solitons that exhibits coherence on the microscopic ("dispersive") scale but is incoherent on the macroscopic ("hydrodynamic") scale. Thus, in contrast to the fully coherent configurations examined in the previous experimental work [23], the soliton now interacts with a *random* nonlinear wave.

SGs have been recently realized in optical experiments and in water wave experiments [30–32]. Nowadays, hydrodynamics and statistics of SGs is an active research area in statistical mechanics [33], mathematical physics [34], and nonlinear physics [35–37] and constitutes a new chapter of turbulence theory, termed integrable turbulence [38].

In our experiment we observe that the nonlinear interaction between a tracer soliton and a finite portion of a dense SG results in the refraction phenomenon similar at a qualitative level to what is observed in ray optics at the interface between two media having different refractive indexes. Unlike the classical refraction of light rays, the observed phenomenon is inherently nonlinear and can be interpreted within the framework of the kinetic theory of SG.

First of all, we measure the macroscopic space shift associated with the solitonic refraction and show that it is quantitatively well described by the IST theory [39–41]. Specifically, we compare the experimentally observed macroscopic position shift Δx acquired by the tracer soliton over a large propagation distance with the "first-principle" IST predictions based on the accumulation of the individual position shifts in pairwise interactions with solitons comprising the SG [42],

$$\Delta x = \sum_j \Delta(\lambda_p, \lambda_j). \tag{1}$$

Here λ_p is the IST spectral parameter of the tracer soliton and $\Delta(\lambda_p, \lambda_j)$ is the position shift of the tracer soliton due to its interaction with the soliton with the spectral parameter λ_j within the SG.

*stephane.randoux@univ-lille.fr

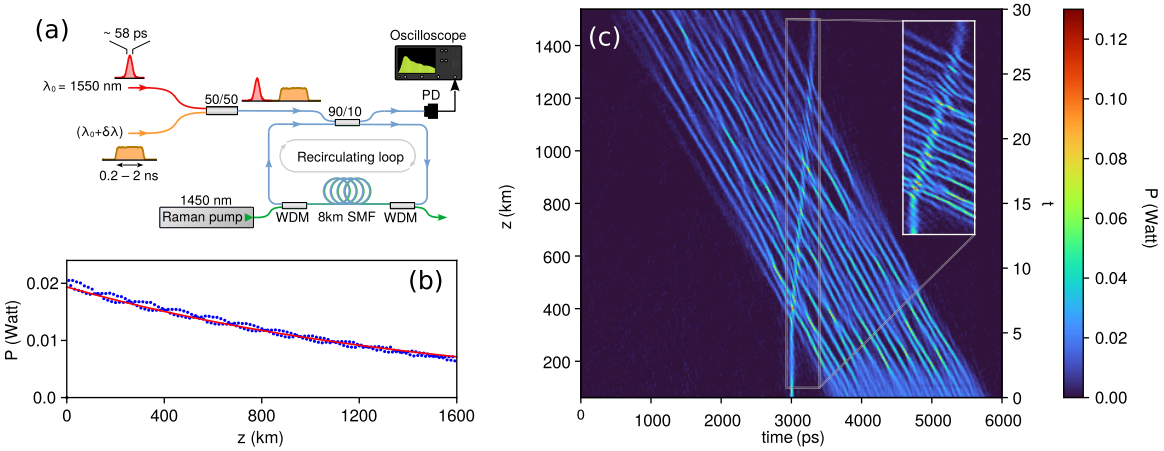

FIG. 1. (a) Schematic representation of the experimental setup. (b) Measured decay (blue points) of the optical power in the recirculating fiber loop. The red line represents an exponential fit of the experimental points, giving a power decay rate of ∼0.0027 dB/km. (c) Typical space-time diagram showing the refraction phenomenon due to the interaction between a tracer soliton and an optical SG forming a bound state. The tracer soliton has a duration of ∼58 ps. It is shifted by ∼280 ps due to its interaction with the optical SG that has a duration of ∼2 ns. The secondary (right) vertical axis shows the normalized evolution time defined as $t = \gamma P_0 z/2 = z/(2L_{NL})$, where $L_{NL} \sim 26.5$ km.

Second, following the approach prescribed by the spectral kinetic theory of SGs [43–45], we measure the effective velocity of the tracer soliton propagating through the SG. From the physical perspective, the effective adjustment of the soliton velocity due to the interaction with the SG is described by the *collision rate ansatz* (CRA) that extrapolates the properties of two-soliton interactions to dense macroscopic ensembles of solitons, in which solitons never separate to exhibit individual short-range interactions. We compare quantitatively the experimental and theoretical values of the effective velocity of the tracer soliton interacting with the dense SG. This comparison represents a crucial step in the physical validation of the CRA and, ultimately, the kinetic theory of SGs as is explained below.

Our experimental setup is schematically shown in Fig. 1(a). It consists of a recirculating fiber loop already used in Refs. [46–48] for some experimental investigations of the nonlinear stage of modulational instability of a plane wave. The recirculating fiber loop is made up of ∼8 km of single-mode fiber (SMF) closed on itself by a 90/10 fiber coupler. The coupler is arranged in such a way that 90% of the intracavity power is recirculated. The optical signal (a tracer soliton plus a SG) circulates in the clockwise direction. At each round trip, 10% of the circulating power is extracted and directed toward a photodetector (PD) coupled to a sampling oscilloscope (160 GSa/s) leading to an overall 32-GHz detection bandwidth. Experimental data are subsequently processed numerically to construct single-shot space-time diagrams showing the wave-field dynamics. The losses accumulated over one circulation in the fiber loop are partially compensated using a counterpropagating Raman pump coupled in and out of the loop via wavelength division multiplexers (WDMs). As shown in Fig. 1(b), this reduces the effective power decay rate of the circulating field to $\alpha_{\text{eff}} \sim 6.2 \times 10^{-4}$ km^{-1} or, equivalently, ∼0.0027 dB/km.

The optical signal propagating inside the fiber loop is composed by a pulse with a duration of ∼58 ps followed by an optical SG initially in the form of a "long" square pulse perturbed by some optical noise [see Figs. 1(a) and 1(c) together with Supplemental Material [49] for details about the generation of light signals]. The short pulse is initially well separated from the square pulse that evolves into a fully randomized bound state SG [30,50–52]. The short pulse and the optical SG have slightly different group velocities, resulting in collisions/interactions between the SG and pulse starting from propagation distances of ∼350–400 km. In practice, the group-velocity difference δv_g between the pulse and the optical SG is realized by using two laser fields with wavelengths that are slightly detuned by $\delta\lambda \simeq 0.125$ nm, resulting in $[\delta v_g]^{-1} \simeq -2.16$ ps/km (see Supplemental Material [49]).

The refraction effect evidenced in Fig. 1(c) is associated with a significant shift (∼280 ps) of the position of the soliton at the spatial coordinate ($z \sim 1200$ km) from which its emerges from the SG. The inset in Fig. 1(c) clearly shows that the velocity of the tracer soliton has slightly changed after is has been transmitted through the SG. This velocity change arises from the fact that the observed dynamics is not perfectly integrable due to the presence of small dissipation in the experiment (see Supplemental Material [49]).

The optical signal circulating in the fiber loop is not only composed of one pulse and one SG but also of a periodic train of 29 short pulses, each pulse being followed by "its own SG" (see Supplemental Material [49] showing the whole experimental pattern recorded in a single shot). The short pulses are all designed to be identical but, in practice, their peak power is $P_p = 39.2 \pm 5.54$ mW and their duration is $\Delta T = 58 \pm 16$ ps (full width at half maximum). The SGs have the initial form of square boxes with a mean power of $P_{\text{SG}} = 19.2 \pm 1.6$ mW. Their duration increases monotonically from ∼200 to ∼2000 ps in 29 steps. Using this strategy, we capture in one single shot the space-time evolution of a set of 29 experiments where we observe the interaction between a pulse and optical SGs with increasing extents.

Figure 2 shows a selection of four experiments from the set of 29 experiments available. Whatever the initial extent of the optical SG, the solitonic refraction phenomenon is

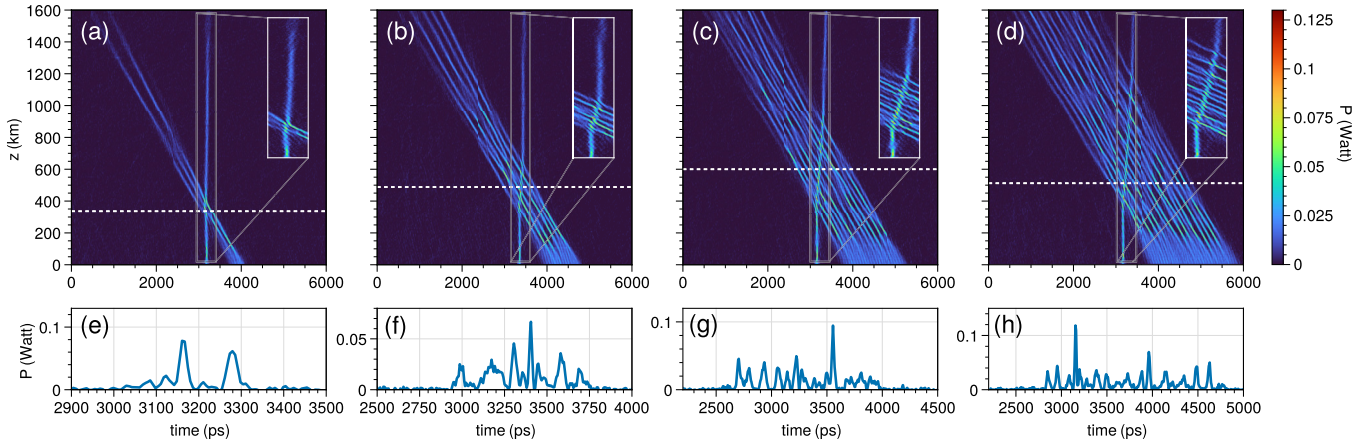

FIG. 2. (a)–(d) Selected set of four space-time diagrams among the 29 available in one single experiment. The shift experienced by the tracer soliton grows with the initial size (duration) of the optical SGs. (e)–(h) Time evolution of the optical power at selected positions (indicated by the horizontal white dashed lines in the top row) where tracer solitons interact with the SGs.

observed. The insets in Figs. 2(a)–2(d) show that the time shift experienced by the soliton increases with the duration of the optical SG. Figures 2(e)–2(h) show the time signal measured at some selected propagation distances, when the tracer solitons interact with the SGs. Figures 2(g) and 2(h) show that the tracer soliton may reach a peak power ∼3 times greater than its initial peak power (∼39 mW) due to its interaction with the SG.

Now we compare the shift measured in the experiment with numerical simulations and the results from the IST theory. As show in Refs. [46–48], dynamical features observed in our recirculating fiber loop can be quantitatively well described by the following 1D-NLSE with a small linear damping:

$$i\frac{\partial A}{\partial z} = \frac{\beta_2}{2}\frac{\partial^2 A}{\partial T^2} - \gamma|A|^2 A - i\frac{\alpha_{\rm eff}}{2}A. \tag{2}$$

$A(z,T)$ represents the complex envelope of the electric field that slowly varies in physical space z and time T. The Kerr coefficient of the fiber is $\gamma = 1.3\ \mathrm{W}^{-1}\ \mathrm{km}^{-1}$. The group velocity dispersion coefficient is $\beta_2 = -22\ \mathrm{ps}^2\ \mathrm{km}^{-1}$.

For a straightforward comparison with the IST theory, we use the following dimensionless form of the focusing 1D-NLSE:

$$i\psi_t + \psi_{xx} + 2|\psi|^2\psi + i\epsilon\psi = 0, \tag{3}$$

which is obtained from Eq. (2) using the following transformations: $\psi = A/\sqrt{P_0}$, $x = T\sqrt{\gamma P_0/|\beta_2|}$, $t = \gamma P_0 z/2$, and $\epsilon = \alpha_{\rm eff}/(\gamma P_0)$. The value $P_0 = 29$ mW has been measured in an annex calibration experiment (see Supplemental Material [49]). Using the canonical expression of the 1D-NLSE given by Eq. (3), the maximum evolution time in normalized units is as large as ∼30 [see the secondary evolution axis in Fig. 1(c)], which corresponds to a propagation over 60 nonlinear lengths with the nonlinear length being defined as $L_{\rm NL} = 1/(\gamma P_0) \simeq 26.5$ km.

The initial condition chosen for approximating the experimental field reads

$$\psi(x, t=0) = \psi_p(x) + \psi_{\rm SG}(x - x_0)\, e^{-ivx/2}, \tag{4}$$

where $\psi_p(x)$ describes the short pulse and $\psi_{\rm SG}(x)$ describes the SG that has a group velocity of $v = 2|\delta v_g|^{-1}/(|\beta_2|\gamma P_0)^{1/2} \simeq 4.74$ with respect to the short pulse in the (x,t) plane.

In the IST theory of the integrable focusing 1D-NLSE (with $\epsilon \equiv 0$), the short pulse (respectively, the SG) is characterized by an area (or L_1 norm) defined as $\mathcal{A}_P = \int |\psi_p(x)|dx$ (respectively, $\mathcal{A}_{\rm SG} = \int |\psi_{\rm SG}(x)|dx$) that determines the number of discrete eigenstates (or solitonic modes) that are embedded in the pulse (respectively, the SG) [12]. In the experiment, $\mathcal{A}_P$ and $\mathcal{A}_{\rm SG}$ are measured with good accuracy. However, the phase of the complex fields $\psi_P(x)$ and $\psi_{\rm SG}(x)$ is not measured, which means that the discrete IST eigenvalues associated with the pulse and the SG cannot be measured. However, the discrete eigenvalues can be estimated using some reasonable assumptions about the analytical expressions for $\psi_P(x)$ and $\psi_{\rm SG}(x)$.

For each of the 29 experiments realized in a single shot, we compute the complex discrete eigenvalue $\lambda_p = i\eta_p$ (and c.c.) ($i^2 = -1$, $\eta_p > 0$) associated with the short pulse by assuming that it can be approximated by $\psi_p(x) = a\,\exp[-x^2/(2w^2)]$, where the parameters a and w are determined using a best-fit procedure constrained by the fact that the integral $\int |\psi_P(x)|dx$ must be equal to the area $\mathcal{A}_P$ measured in the experiment. Applying the same procedure for the SG, we compute an ensemble of N discrete eigenvalues $\lambda_j = i\eta_j - v/4$ (and c.c.) ($j = 1, \ldots, N$, $\eta_j > 0$) by assuming that the initial box can be approximated by $\psi_{\rm SG}(x) = b\,\exp[-x^{2n}/(2L^{2n})]$, where the real parameters b, x_0, and L and the integer parameter n are determined using a best-fit procedure constrained by the fact that the integral $\int |\psi_{\rm SG}(x)|dx$ must be equal to the area $\mathcal{A}_{\rm SG}$ measured in each of the 29 experiments.

Figure 3(a) compares the space shift Δx measured in the experiment with the IST formula (1) which assumes the form

$$\Delta x = \frac{1}{\eta_p}\sum_{j=1}^{N} \ln\left|\frac{i\eta_p + i\eta_j + v/4}{i\eta_p - i\eta_j + v/4}\right| \tag{5}$$

on using the well-known expression for the elementary position shift $\Delta(\lambda_p, \lambda_j) = (1/\mathrm{Im}\lambda_p)\ln|\frac{\lambda_p - \lambda_j^*}{\lambda_p - \lambda_j}|$ in the 1D-NLSE two-soliton interaction [42]. Importantly, the spatial shift arising from the interaction between the tracer soliton and the

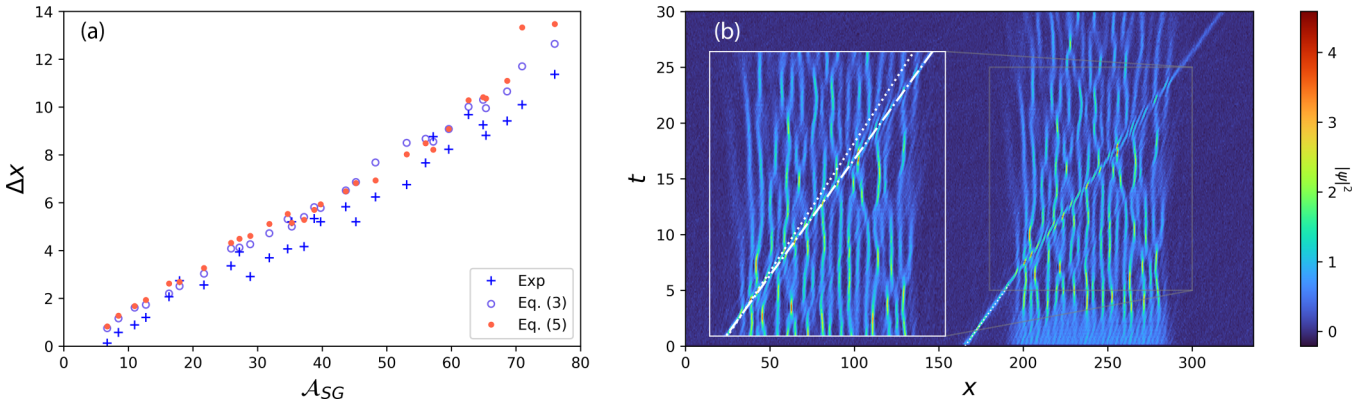

FIG. 3. Comparison between experimental results and theoretical results from the IST theory and the kinetic theory of SG. (a) Shifts measured in the experiment (blue crosses), in numerical simulations of Eq. (3) (empty circles) and using Eq. (5) (solid circles). (b) Space-time diagram showing the interaction between the tracer soliton and the dense SG composed of 24 solitons in the reference frame moving at the group velocity of the SG. The dashed white line following the trajectory of the tracer soliton inside the optical SG has the slope $1/s(\eta_p) \simeq 1/5.26 \simeq 0.19$ predicted by the kinetic theory of SGs [Eqs. (6)–(8)].

radiative modes composing the box is neglected in Eq. (5) [39–41].

As shown in Fig. 3(a), a good quantitative agreement is obtained between experiment (blue crosses) and Eq. (5) (solid circles). This agreement is slightly improved in numerical simulations of Eq. (3) (empty circles) because these simulations incorporate the correction to the spatial shift due to the presence of radiative modes in the square boxes. Note that the spatial shift Δx is defined in the IST theory as an asymptotic quantity determined at infinite evolution time when the interaction between the tracer soliton and other solitons is negligible. In the experiment, the presence of small dissipation breaks the integrability condition inherent in the IST theory and the spatial shift must be measured at finite evolution time. We have measured the spatial shift at the point where the tracer soliton emerges from the SG (see Supplemental Material [49]). Despite this limitation, our results show that the shift described by Eq. (5) is robust to the presence of small perturbative effects.

Along with the macroscopic spatial shift, the nonlinear interaction between the tracer soliton and the SG results in a discernible change in the soliton propagation velocity. From the perspective of the SG kinetic theory [43–45] the effective velocity $s(\lambda_p)$ of a tracer soliton propagating through a SG is given by the following *equation of state*:

$$s(\lambda_p) = s_0(\lambda_p) + \int_\Gamma \Delta(\lambda_p, \zeta) f(\zeta)[s(\lambda_p) - s(\zeta)] d\xi d\mu. \quad (6)$$

Here $s_0(\lambda_p) = -4\mathrm{Re}\lambda_p$ is the velocity of the noninteracting (free) tracer soliton and $f(\zeta)$ is the *density of states* (DOS) of the SG—the distribution function of solitons with respect to the spectral parameter $\zeta = \xi + i\mu \in \Gamma \subset \mathbb{C}$ [32,43–45,50]. The equation of state is a direct consequence of the so-called CRA, a fundamental principle that provides the link between micro- and macroscopic properties of SGs [45]. It is also at the heart of generalized hydrodynamics—the hydrodynamic theory of many-body quantum and classical integrable systems [53,54], whose intimate connection with the kinetic theory of soliton gases has been recently established [33]. While the validity of the CRA has been mathematically proven for KdV and 1D-NLSE SGs via the asymptotic (thermodynamic) limit of multiphase nonlinear wave solutions [44,55], its experimental verification is lacking. Such a verification is crucial for the justification of the physical validity of the kinetic theory of soliton gases.

Applied to the configuration of our experiment and written in the reference frame associated with the SG [so that $s_0(\lambda_p) = v, s(\zeta) \equiv 0, \zeta = i\mu \in \Gamma = [0, ib], \lambda_p = i\eta_p - v/4$], the equation of state (6) yields the following for the tracer soliton velocity:

$$s(\eta_p) = \frac{v}{1 - \frac{1}{\eta_p}\int_0^b \ln\left|\frac{i\eta_p + i\mu + v/4}{i\eta_p - i\mu + v/4}\right| f(\mu) d\mu}. \quad (7)$$

As discussed in Ref. [50], nonlinear wave fields in a dense SG evolving from the box initial data has the DOS given by $f(\mu) = \mu/(\pi\sqrt{b^2 - \mu^2})$, $\mu \in [0, b)$. For such DOS the integral in Eq. (7) can be evaluated explicitly to give [44]

$$s(\eta_p) = \frac{v\eta_p}{\mathrm{Im}\sqrt{b^2 - \eta_p^2 + \frac{v^2}{16} + i\frac{\eta_p v}{2}}}. \quad (8)$$

Considering one of the SGs of the largest extent ($\mathcal{A}_{\mathrm{SG}} = 71$, $b = 0.603$) interacting with the pulse having spectral parameters $\eta_p = 0.617$ and $v = 4.74$ [see Fig. 1(c)], Eq. (8) predicts that the velocity of the tracer soliton in the interaction region is $s(\eta_p) = 5.26$, which represents a relative velocity change, $[s(\eta_p) - v]/v$, of $\sim$11%. This velocity change is indeed quantitatively measured in the experiment. This is illustrated in Fig. 3(b) where the dashed line parallel to the trajectory followed by the tracer soliton inside the SG has indeed the slope $1/s(\eta_p) \simeq 1/5.26 \simeq 0.19$ that is predicted by the kinetic theory of SGs.

In conclusion, we reported an experiment allowing one to investigate the interaction between a soliton and an optical SG. The observables of this interaction—the macroscopic spatial shift of the tracer soliton and its effective velocity—are favorably compared with the theoretical predictions of the IST theory and of the kinetic theory of SGs. These comparisons provide an important step towards the physical validation

of the fundamental theoretical principles behind the spectral theory of SGs.

ACKNOWLEDGMENTS

This work has been partially supported by the Agence Nationale de la Recherche through the StormWave (Grant No. ANR-21-CE30-0009) and SOGOOD (Grant No. ANR-21-CE30-0061) projects, the LABEX CEMPI project (Grant No. ANR-11-LABX-0007), the Ministry of Higher Education and Research, the Hauts de France Council, and the European Regional Development Fund (ERDF) through the Nord-Pas de Calais Regional Research Council and the European Regional Development Fund (ERDF) through the Contrat de Projets Etat-Région (CPER Photonics for Society P4S). The authors thank the Isaac Newton Institute for Mathematical Sciences for support and hospitality during the programme "Dispersive Hydrodynamics: Mathematics, Simulation and Experiments, with Applications in Nonlinear Waves" when part of the work on this paper was undertaken. G.E.'s and G.R.'s work was also supported by EPSRC Grant No. EP/W032759/1. G.R. thanks the Simons Foundation for partial support.

[1] A. Hasegawa and Y. Kodama, *Solitons in Optical Communications*, Oxford Series in Optical and Imaging Sciences (Clarendon, Oxford, 1995).

[2] J. H. V. Nguyen, P. Dyke, D. Luo, B. A. Malomed, and R. G. Hulet, Collisions of matter-wave solitons, Nat. Phys. **10**, 918 (2014).

[3] D. Luo, Y. Jin, J. H. V. Nguyen, B. A. Malomed, O. V. Marchukov, V. A. Yurovsky, V. Dunjko, M. Olshanii, and R. G. Hulet, Creation and characterization of matter-wave breathers, Phys. Rev. Lett. **125**, 183902 (2020).

[4] H. C. Yuen and B. M. Lake, Nonlinear deep water waves: Theory and experiment, Phys. Fluids **18**, 956 (1975).

[5] S. Trillo, G. Deng, G. Biondini, M. Klein, G. F. Clauss, A. Chabchoub, and M. Onorato, Experimental observation and theoretical description of multisoliton fission in shallow water, Phys. Rev. Lett. **117**, 144102 (2016).

[6] B. Deng, J. R. Raney, V. Tournat, and K. Bertoldi, Elastic vector solitons in soft architected materials, Phys. Rev. Lett. **118**, 204102 (2017).

[7] T. Heimburg and Andrew D. Jackson, On soliton propagation in biomembranes and nerves, Proc. Natl. Acad. Sci. USA **102**, 9790 (2005).

[8] M. J. Ablowitz, D. J. Kaup, A. C. Newell, and H. Segur, Nonlinear-evolution equations of physical significance, Phys. Rev. Lett. **31**, 125 (1973).

[9] N. J. Zabusky and M. D. Kruskal, Interaction of "solitons" in a collisionless plasma and the recurrence of initial states, Phys. Rev. Lett. **15**, 240 (1965).

[10] S. P. Novikov, S. V. Manakov, L. P. Pitaevskii, and V. E. Zakharov, *Theory of Solitons: The Inverse Scattering Method* (Springer, Berlin, 1984).

[11] M. Remoissenet, *Waves Called solitons: Concepts and Experiments*, 2nd ed. (Springer, Berlin, 1996).

[12] J. Yang, *Nonlinear Waves in Integrable and Non-integrable Systems*, Mathematical Modeling and Computation (Society for Industrial and Applied Mathematics, Philadelphia, 2010).

[13] H. Ikezi, R. J. Taylor, and D. R. Baker, Formation and interaction of ion-acoustic solitions, Phys. Rev. Lett. **25**, 11 (1970).

[14] D. W. Aossey, S. R. Skinner, J. L. Cooney, J. E. Williams, M. T. Gavin, D. R. Andersen, and K. E. Lonngren, Properties of soliton-soliton collisions, Phys. Rev. A **45**, 2606 (1992).

[15] A. Slunyaev, M. Klein, and G. F. Clauss, Laboratory and numerical study of intense envelope solitons of water waves: Generation, reflection from a wall, and collisions, Phys. Fluids **29**, 047103 (2017).

[16] F. M. Mitschke and L. F. Mollenauer, Experimental observation of interaction forces between solitons in optical fibers, Opt. Lett. **12**, 355 (1987).

[17] F. Xin, F. Di Mei, L. Falsi, D. Pierangeli, C. Conti, A. J. Agranat, and E. DelRe, Evidence of chaotic dynamics in three-soliton collisions, Phys. Rev. Lett. **127**, 133901 (2021).

[18] P. A. Andrekson, N. A. Olsson, P. C. Becker, J. R. Simpson, T. Tanbun-Ek, R. A. Logan, and K. W. Wecht, Observation of multiple wavelength soliton collisions in optical systems with fiber amplifiers, Appl. Phys. Lett. **57**, 1715 (1990).

[19] J. S. Aitchison, A. M. Weiner, Y. Silberberg, D. E. Leaird, M. K. Oliver, J. L. Jackel, and P. W. E. Smith, Experimental observation of spatial soliton interactions, Opt. Lett. **16**, 15 (1991).

[20] M. Shalaby, F. Reynaud, and A. Barthelemy, Experimental observation of spatial soliton interactions with a $\pi/2$ relative phase difference, Opt. Lett. **17**, 778 (1992).

[21] N. G. Parker, A. M. Martin, S. L. Cornish, and C. S. Adams, Collisions of bright solitary matter waves, J. Phys. B: At., Mol. Opt. Phys. **41**, 045303 (2008).

[22] S. Stellmer, C. Becker, P. Soltan-Panahi, E.-M. Richter, S. Dörscher, M. Baumert, J. Kronjäger, K. Bongs, and K. Sengstock, Collisions of dark solitons in elongated bose-einstein condensates, Phys. Rev. Lett. **101**, 120406 (2008).

[23] M. D. Maiden, D. V. Anderson, N. A. Franco, G. A. El, and M. A. Hoefer, Solitonic dispersive hydrodynamics: Theory and observation, Phys. Rev. Lett. **120**, 144101 (2018).

[24] P. Sprenger, M. A. Hoefer, and G. A. El, Hydrodynamic optical soliton tunneling, Phys. Rev. E **97**, 032218 (2018).

[25] G. Biondini, S. Li, and D. Mantzavinos, Soliton trapping, transmission, and wake in modulationally unstable media, Phys. Rev. E **98**, 042211 (2018).

[26] G. Biondini and J. Lottes, Nonlinear interactions between solitons and dispersive shocks in focusing media, Phys. Rev. E **99**, 022215 (2019).

[27] K. van der Sande, G. A. El, and M. A. Hoefer, Dynamic soliton-mean flow interaction with non-convex flux, J. Fluid Mech. **928**, A21 (2021)

[28] A. Mucalica and D. E. Pelinovsky, Solitons on the rarefaction wave background via the Darboux transformation, Proc. R. Soc. A: Math., Phys. and Eng. Sci. **478**, 20220474 (2022).

[29] M. J. Ablowitz, J. T. Cole, G. A. El, M. A. Hoefer, and Xudan Luo, Soliton-mean field interaction in Korteweg-de Vries dispersive hydrodynamics, arXiv:2211.14884.

[30] G. Marcucci, D. Pierangeli, A. J. Agranat, R.-K. Lee, E. DelRe, and C. Conti, Topological control of extreme waves, Nat. Commun. **10**, 5090 (2019).

[31] I. Redor, E. Barthélemy, H. Michallet, M. Onorato, and N. Mordant, Experimental evidence of a hydrodynamic soliton gas, Phys. Rev. Lett. **122**, 214502 (2019).

[32] P. Suret, A. Tikan, F. Bonnefoy, F. Copie, G. Ducrozet, A. Gelash, G. Prabhudesai, G. Michel, A. Cazaubiel, E. Falcon, G. El, and S. Randoux, Nonlinear spectral synthesis of soliton gas in deep-water surface gravity waves, Phys. Rev. Lett. **125**, 264101 (2020).

[33] T. Bonnemain, B. Doyon, and G. El, Generalized hydrodynamics of the KdV soliton gas, J. Phys. A: Math. Theor. **55**, 374004 (2022).

[34] M. Girotti, T. Grava, R. Jenkins, K. T.-R. McLaughlin, and A. Minakov, Soliton versus the gas: Fredholm determinants, analysis, and the rapid oscillations behind the kinetic equation, Comm. Pure Appl. Math. (2023), doi:10.1002/cpa.22106.

[35] I. Redor, H. Michallet, N. Mordant, and E. Barthélemy, Experimental study of integrable turbulence in shallow water, Phys. Rev. Fluids **6**, 124801 (2021).

[36] A. V. Slunyaev and T. V. Tarasova, Statistical properties of extreme soliton collisions, Chaos **32**, 101102 (2022).

[37] E. Pelinovsky and E. Shurgalina, *KDV Soliton Gas: Interactions and Turbulence* (Springer, Cham, 2017), pp. 295–306.

[38] V. E. Zakharov, Turbulence in integrable systems, Stud. Appl. Math. **122**, 219 (2009).

[39] L. Martínez Alonso, Soliton motion in the case of a nonzero reflection coefficient, Phys. Rev. Lett. **54**, 499 (1985).

[40] L. Martínez Alonso, Effect of the radiation component on soliton motion, Phys. Rev. D **32**, 1459 (1985).

[41] M. Borghese, R. Jenkins, and K. D. T.-R. McLaughlin, Long time asymptotic behavior of the focusing nonlinear Schrödinger equation, Ann. Inst. Henri Poincaré C, Anal. non linéaire **35**, 887 (2018).

[42] V. E. Zakharov and A. B. Shabat, Exact theory of two-dimensional self-focusing and one-dimensional self-modulation of waves in nonlinear media, Sov. Phys. JETP **34**, 62 (1972).

[43] G. A. El and A. M. Kamchatnov, Kinetic equation for a dense soliton gas, Phys. Rev. Lett. **95**, 204101 (2005).

[44] G. El and A. Tovbis, Spectral theory of soliton and breather gases for the focusing nonlinear Schrödinger equation, Phys. Rev. E **101**, 052207 (2020).

[45] G. A. El, Soliton gas in integrable dispersive hydrodynamics, J. Stat. Mech.: Theory Exp. (2021) 114001.

[46] A. E. Kraych, P. Suret, G. El, and S. Randoux, Nonlinear evolution of the locally induced modulational instability in fiber optics, Phys. Rev. Lett. **122**, 054101 (2019).

[47] A. E. Kraych, D. Agafontsev, S. Randoux, and P. Suret, Statistical properties of the nonlinear stage of modulation instability in fiber optics, Phys. Rev. Lett. **123**, 093902 (2019).

[48] F. Copie, P. Suret, and S. Randoux, Spatiotemporal observation of higher-order modulation instability in a recirculating fiber loop, Opt. Lett. **47**, 3560 (2022).

[49] See Supplemental Material at http://link.aps.org/supplemental/10.1103/PhysRevResearch.5.L042002 for details about the experimental setup together with some discussions about the influence of the strength of the initial noise and the analogy between soliton refraction and refraction of light rays, which includes Refs. [12,47].

[50] A. Gelash, D. Agafontsev, V. Zakharov, G. El, S. Randoux, and P. Suret, Bound state soliton gas dynamics underlying the spontaneous modulational instability, Phys. Rev. Lett. **123**, 234102 (2019).

[51] F. Bonnefoy, A. Tikan, F. Copie, P. Suret, G. Ducrozet, G. Prabhudesai, G. Michel, A. Cazaubiel, E. Falcon, G. El, and S. Randoux, From modulational instability to focusing dam breaks in water waves, Phys. Rev. Fluids **5**, 034802 (2020).

[52] G. A. El, E. G. Khamis, and A. Tovbis, Dam break problem for the focusing nonlinear Schrödinger equation and the generation of rogue waves, Nonlinearity **29**, 2798 (2016).

[53] B. Doyon, T. Yoshimura, and J.-S. Caux, Soliton gases and generalized hydrodynamics, Phys. Rev. Lett. **120**, 045301 (2018).

[54] B. Doyon, Lecture notes on generalised hydrodynamics, SciPost Phys. Lect. Notes **18**, (2020).

[55] G. A. El, The thermodynamic limit of the Whitham equations, Phys. Lett. A **311**, 374 (2003).